LANGMUIR

Article

pubs.acs.org/Langmuir

# Direct Functionalization of an Acid-Terminated Nanodiamond with Azide: Enabling Access to 4-Substituted-1,2,3-Triazole-Functionalized Particles

Zachary C. Kennedy, Christopher A. Barrett, and Marvin G. Warner*

Signatures Science & Technology Division, National Security Directorate, Pacific Northwest National Laboratory, P.O. Box 999, Richland, Washington 99352, United States

Supporting Information

**ABSTRACT:** Azides on the periphery of nanodiamond materials (ND) are of great utility because they have been shown to undergo Cu-catalyzed and Cu-free cycloaddition reactions with structurally diverse alkynes, affording particles tailored for applications in biology and materials science. However, current methods employed to access ND featuring azide groups typically require either harsh pretreatment procedures or multiple synthesis steps and use surface linking groups that may be susceptible to undesirable cleavage. Here we demonstrate an alternative single-step approach to producing linker-free, azide-functionalized ND. Our method was applied to low-cost, detonation-derived ND powders where surface carbonyl groups undergo silver-mediated decarboxylation and radical substitution with azide. ND with directly grafted azide groups were then treated with a variety of aliphatic, aromatic, and fluorescent alkynes to afford 1-(ND)-4-substituted-1,2,3-triazole materials under standard copper-catalyzed cycloaddition conditions. Surface modification steps were verified by characteristic infrared absorptions and elemental analyses. High loadings of triazole surface groups (up to 0.85 mmol $g^{-1}$) were obtained as determined from thermogravimetric analysis. The azidation procedure disclosed is envisioned to become a valuable initial transformation in numerous future applications of ND.

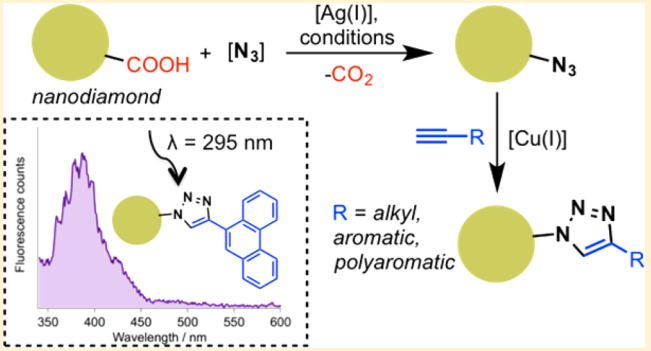


## INTRODUCTION

Diamond is a promising material on the nanoscale because of its robust mechanical properties, high thermal conductivity,[1] and electrical resistivity as well as its potential to hold permanently fluorescent color centers (such as nitrogen vacancies (NVs)).[2] Furthermore, the diamond allotrope of carbon has extremely high chemical stability and resistance to degradation in harsh environments. Coupled with this stability, the nanodiamond (ND) class of materials (larger, polydisperse mixtures unlike that of chemically uniform nanodiamonds or diamondoids)[3] has a carbon surface that may be chemically modified to feature a variety of functional groups.[4] ND synthesized by detonation, the most commonly used and cheapest method (estimated to be as low as $96/kg in 2010),[5] yields 4−5 nm primary particles that are typically isolated on an industrial scale by thermal oxidation in air and/or with concentrated acids.[6] These treatments remove a large degree of noncarbon and nondiamond carbon impurities. The detonation nanodiamond (dND) surface after purification is terminated primarily by carboxylic acid groups.[7] Because of their low production cost and the breadth of reactivity of carboxylic acids, acid-functionalized dND is an attractive starting material for further surface modification.

Carboxylic acid-dND has been previously outlined to undergo many transformations to enhance particle interactions with biomolecules,[8,9] metal ions,[10] and other nanostructures.[11] The most common synthesis modifications of dND are the conversion of carboxyl groups to alcohol by reduction using borane or $LiAlH_4$,[12] to acid chloride by thionyl chloride,[13] and to amides by amines[9] as well as aggressive transformations by high-temperature amination,[14] fluorination,[15] or photochemical chlorination.[16] Recently, a surge of reports on the silver-catalyzed decarboxylation of $C(sp^3)$-COOH bonds on small molecules have emerged to specifically introduce an array of valuable functional groups directly (aryl sulfide,[17] alkyne,[18] fluorine,[19] allyl,[20] etc.). Using this functionalization strategy, high-temperature, high-pressure (HPHT) ND have recently been shown to undergo decarboxylation and fluorination using Ag(I) and Selectfluor, a significantly safer method for installing fluorine than was previously reported.[21] Inspired by the simplicity of these approaches (mild heating, aqueous solution, commercially available reagents), we aimed to further investigate Ag(I)-mediated decarboxylation as a method to

**Received:** December 13, 2016
**Revised:** February 3, 2017
**Published:** March 1, 2017





DOI: 10.1021/acs.langmuir.6b04477
*Langmuir* XXXX, XXX, XXX−XXX

transform the surface of COOH-dND to contain functional groups of high general utility.

Of particular relevance was the reported conversion of aliphatic carboxylic acid to azide (Scheme 1a).[22,23] A closely

**Scheme 1. (a) Silver-Catalyzed Decarboxylative Azidation of Diamondoid Adamantane-COOH, (b) Primary Methods to Produce Azide-dND to Date, and (c) the Application of Silver-Mediated Decarboxylative Azidation to dND**

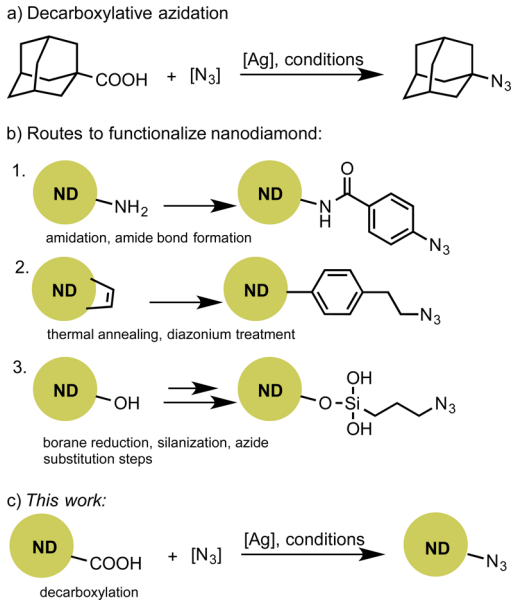


related classical transformation is the Hunsdieker reaction involving the reaction of a Ag carboxylic acid salt with a halogen (azide is known as a pseudohalide) to yield a halide.[24] Azides are a versatile functional group that participate in reactions essential to applications in materials science and chemical biology. Specifically, organic azides are famously known for their roles in the click Staudinger ligation[25] and ubiquitous azide−alkyne Huisgen cycloaddition reactions.[26] Three primary routes to producing azide-functionalized dND have previously been established (Scheme 1b). The first route involves ND aminolysis followed by amide bond formation at the surface using carbodiimide activation and treatment with an aromatic carboxylic acid containing a terminal azide group.[27] Amide-dND's are thus simple to produce; however, amide bond linkages may be susceptible to hydrolysis. The second approach involves high-temperature annealing to generate $sp^2$ carbon at the surface of dND and treatment with an aromatic diazonium salt containing an azide group.[28] This method is also straightforward but does require heating the particles to 750 °C in vacuum. Furthermore, the azide groups were noted to be susceptible to cleavage during subsequent cycloaddition reactions. Finally, borane-reduced dND may be converted to silanol with omega azide termination.[29] A relatively homogeneous starting ND−OH material enables the efficient surface loading of azide; however, this approach comprises multiple steps and uses silanes, which may undergo undesirable cross-linking or hydrolysis. Furthermore, all three routes necessitate the use of spacer groups between the ND surface and azide group. We aimed to develop an alternative method to produce robust azide-dND without a surface linker.

Herein, we apply silver-mediated decarboxylation for the solution-phase azidation of carboxylic acid-functionalized dND. The combination of Ag(I) as a catalyst from $AgNO_3$ or AgF and potassium persulfate as an oxidant facilitates the decarboxylation of ND carboxyl groups, followed by a radical substitution for azide directly at the surface using a tosyl azide source. The azidation procedure occurred in a mixed aqueous−acetonitrile mixture with only mild heating. To illustrate the utility of ND functionalized using this method, azide-ND materials were treated with aliphatic and aromatic alkynes to yield triazole adducts under Cu-catalyzed conditions. We report high surface loadings of (4-substituted)-1,2,3-triazole groups on dND, achieved when the azide starting material was synthesized using AgF mediation. The 1,2,3-triazole-functionalized particles also represent, to our knowledge, the first direct triazole surface termination of ND.

## EXPERIMENTAL METHODS

**Materials and Methods.** Manipulations were performed in air unless otherwise stated. Carboxylic acid-functionalized detonation nanodiamond (**1**) with a reported primary particle size of 4−5 nm (corroborated by TEM, Figure 2C), ∼130 nm aggregate size, and a 0.6% ash content was purchased from Adámas Nanotechnologies (Raleigh, NC, USA). All other solvents and reagents were purchased from commercial sources (typically Sigma-Aldrich or TCI).

Bath sonication was performed using a Branson 2510 and sonication by an ultrasonic horn using a Hielscher UP50H. FT-IR analysis of ND samples was performed on a Thermo Nicolet 6700 by mixing dried ND powders into KBr and pressing into pellets. Thermogravimetric analysis (TGA) was performed on a Netzsch TG 209 F3 in $Al_2O_3$ crucibles. Dried samples (typically 7−8 mg) were initially held at 40 °C for 10 min before heating to 800 °C at a rate of 10 °C $min^{-1}$ in a He atmosphere. Gas adsorption measurements were performed in a $N_2$ atmosphere at 77 K on a Quantachrome Quadrasorb SI. The specific surface area was determined from the Langmuir isotherm using the multipoint Brunauer−Emmett−Teller (BET) method. Elemental analysis was performed by Robertson Microlit Laboratories (Ledgewood, NJ, USA) by combustion analysis for carbon, hydrogen, and nitrogen and by the ion-selective electrode method for fluorine. Transmission electron microscopy (TEM), selected-area electron diffraction (SAED), and energy-dispersive X-ray spectroscopy (EDS) were performed using a Tecnai G2 F20 (FEI Corporation) operating at 200 kV.

**Synthesis Procedures.** *4-Methylbenzenesulfonyl Azide ($TsN_3$).*[30] [***Warning!*** *Caution must be taken when handling sodium azide because of its high acute toxicity.*] 4-Toluenesulfonyl chloride (2.01 g, 10.5 mmol) and sodium azide (872 mg, 13.4 mmol) were dissolved in acetone (40 mL) and $H_2O$ (12 mL). The mixture was stirred at room temperature for 1 h before removing half the reaction volume under reduced pressure. The evaporated solvent was condensed over NaOH pellets to trap any poisonous and explosive $HN_3$ potentially formed. The product was isolated by extraction into ethyl acetate (50 mL), washed with $H_2O$ (2 × 30 mL), dried with $MgSO_4$, and concentrated under reduced pressure to yield $TsN_3$ as a colorless liquid (2.00 g, 96%) that was used without further purification. FT-IR (KBr) $\nu$ ($cm^{-1}$): 3271 (w), 3068 (w), 2925 (w), 2386 (w), 2125 (s, N═N═N), 1925 (w), 1596 (m), 1495 (w), 1450 (w), 1383 (s, $SO_2$ sym), 1308 (w), 1298 (w), 1167 (s, $SO_2$ antisym), 1120 (w), 1086 (s), 1041 (w), 1018 (w), 814 (m), 746 (s), 703 (m), 661 (s), 592 (s), 539 (s), 500 (w). Note that whereas $TsN_3$ is a relatively stable azide, the product was stored at −20 °C to mitigate potential explosive and shock sensitivity hazards.

*Carboxylic Acid-Terminated Detonation Nanodiamond (ND-**1**) (from Adámas Nanotechnologies).* FT-IR (KBr) $\nu$ ($cm^{-1}$): 3435 (s), 2919 (w), 2850 (w), 1763 (w, C═O), 1630 (m, O−H bend; $H_2O$), 1401 (w), 1129 (w). C, 88.49%; H, 0.86%; N, 2.26%. TGA (mass loss ($\Delta m$)) (150−470 °C): 0.5%. Specific surface area by BET: 296 $m^2$ $g^{-1}$.

*Azide Detonation Nanodiamond Using $AgNO_3$ (ND-**2a**).* Carboxylic acid-functionalized detonation nanodiamond (ND-**1**) (299 mg) was suspended in $CH_3CN/H_2O$ (1:1, 30 mL total) in a $N_2$ atmosphere and dispersed by bath sonication for 20 min. $AgNO_3$


DOI: 10.1021/acs.langmuir.6b04477
Langmuir XXXX, XXX, XXX−XXX

(104 mg, $6.1 \times 10^{-4}$ mol), potassium persulfate (323 mg, $1.2 \times 10^{-3}$ mol), and $TsN_3$ (354 mg, $1.8 \times 10^{-3}$ mol) were sequentially added to the solution. The flask was covered with Al foil (to minimize light exposure to $AgNO_3$), heated to 50 °C, and stirred for 18 h. After cooling to room temperature, the mixture was transferred to a centrifuge tube and crude ND was isolated as a pellet by centrifugation (10 000*g* for 5 min). The supernatant was removed and the pellet was washed repeatedly with $H_2O$ (three times) and $CH_3CN$ (two times), followed by isolation by centrifugation (10 000*g* for 5 min) and the removal of the supernatant after each washing step. After the final wash, the NDs were dried extensively under reduced pressure at 45 °C to yield ND-**2** as a gray powder (280 mg). FT-IR (KBr) $\nu$ ($cm^{-1}$): 3432 (s), 2920 (w), 2851 (w), 2134 (w, N═N═N), 1763 (w, C═O), 1630 (m, O−H bend; $H_2O$), 1264 (w), 1169 (w). C, 87.23%; H, 0.76%; N, 2.32%. TGA ($\Delta m$) (150−470 °C): 1.4%.

*Azide Detonation Nanodiamond Using AgF (ND-**2b**).* Carboxylic acid-functionalized detonation nanodiamond (ND-**1**) (299 mg) was suspended in $CH_3CN/H_2O$ (1:1, 30 mL total) in a $N_2$ atmosphere and dispersed by bath sonication for 20 min. AgF (76 mg, $6.0 \times 10^{-4}$ mol), potassium persulfate (327 mg, $1.2 \times 10^{-3}$ mol), and $TsN_3$ (355 mg, $1.8 \times 10^{-3}$ mol) were sequentially added to the solution. The flask was covered with Al foil (to minimize light exposure to AgF), and the mixture was stirred and held at 50 °C for 18 h. After cooling to room temperature, the mixture was transferred to a centrifuge tube and crude ND was isolated as a pellet by centrifugation (10 000*g* for 5 min). The supernatant was removed, and the pellet was washed repeatedly with $H_2O$ (three times) and $CH_3CN$ (two times), followed by isolation by centrifugation (10 000*g* for 5 min) and the removal of the supernatant after each washing step. After the final wash, the NDs were dried extensively under reduced pressure at 45 °C to yield ND-**2** as a gray powder (251 mg). FT-IR (KBr) $\nu$ ($cm^{-1}$): 3432 (s), 2920 (w), 2851 (w), 2136 (m, N═N═N), 1763 (m, C═O), 1630 (m, O−H bend; $H_2O$), 1169 (m), 751 (w), 602 (w), 541 (w), 483 (w). Average of two analyses: C, 86.30%; H, 0.94%; N, 2.55%. TGA ($\Delta m$) (150−470 °C): 1.9%.

**General Procedure for the Synthesis of 1-dND-(4-substituted)-1,2,3-triazoles.** ND-**2b** was suspended in DMF/$H_2O$ (4:1) by bath sonication for 10 min. Alkyne, copper(II) sulfate pentahydrate, and sodium L-ascorbate were then added sequentially. The suspension was stirred at room temperature for 18−24 h. The reaction mixture was transferred to a centrifuge tube and rinsed with water and/or DMF to facilitate a complete transfer. Crude triazole-functionalized dND was separated by centrifugation at 9000*g*. Purification was performed with the sequence of washes listed below, assisted by bath sonication and stirring of the pelleted material at each washing step to remove adsorbed impurities.

*Wash Sequence A.* The supernatant was removed and the pellet was washed repeatedly with 15% $NH_4OH$(aq) (up to five times), 0.1 M HCl(aq), $H_2O$, DMSO, EtOH (two times), and hexanes, followed by isolation by centrifugation (9000*g*) and removal of the supernatant after each washing step. Note that $NH_4OH$ washes were performed until the supernatant no longer had any detectable blue color (from $Cu(NH_3)_4^{2+}$).

*Wash Sequence B.* This sequence was performed according to sequence A but with washes of 15% $NH_4OH$(aq) (up to five times), 0.1 M HCl(aq), $H_2O$, acetone (two times), and hexanes.

*4-((1,2,3-Triazol-4-yl)methoxy)aniline-terminated Nanodiamond (**3b**).* Following the general procedure, ND-**2b** (29 mg) was suspended in DMF/$H_2O$ (4:1, 5 mL total). 4-Aminophenyl propargyl ether (86 mg, $5.8 \times 10^{-4}$ mol), Cu(II)$SO_4 \cdot 5H_2O$ (58 mg, $2.3 \times 10^{-4}$ mol), and sodium L-ascorbate (93 mg, $4.7 \times 10^{-4}$ mol) were added sequentially, and the resulting mixture was stirred at room temperature for 18 h. Particles were purified according to reported wash sequence A and dried in vacuo at 75 °C to yield ND-**3b** as a brownish-gray powder (25 mg). FT-IR (KBr) $\nu$ ($cm^{-1}$): 3436 (s), 2924 (w), 2853 (w), 1752 (w, C═O), 1630 (m, O−H bend; $H_2O$), 1618 (m), 1504 (w, N−H; $NH_3^+$), 1400 (w), 1385 (w), 1262 (w), 1023 (w). TGA ($\Delta m$) (150−470 °C): 4.3%. C, 80.19%; H, 1.13%; N, 2.63%.

*(1,2,3-Triazol-4-yl)methanol-Terminated Nanodiamond (**4b**).* Following the general procedure, ND-**2b** (30 mg) was suspended in DMF/$H_2O$ (4:1, 5 mL total). Propargyl alcohol (34 mg, $6.0 \times 10^{-4}$ mol), Cu(II)$SO_4 \cdot 5H_2O$ (59 mg, $2.4 \times 10^{-4}$ mol), and sodium L-ascorbate (95 mg, $4.8 \times 10^{-4}$ mol) were added sequentially, and the resulting mixture was stirred at room temperature for 22 h. Particles were purified according to reported wash sequence A and dried in vacuo at 75 °C to yield ND-**4b** as a gray powder (17 mg). FT-IR (KBr) $\nu$ ($cm^{-1}$): 3436 (s), 2920 (w), 2851 (w), 1752 (w, C═O), 1630 (m, O−H bend; $H_2O$), 1401 (w), 1020 (w, C−O), 953 (w). TGA ($\Delta m$) (150−470 °C): 4.9%. C, 80.32%; H, 1.09%; N, 2.10%.

*4-Butyl-1H-1,2,3-triazole-Terminated Nanodiamond (**5b**).* Following the general procedure, ND-**2b** (30 mg) was suspended in DMF/$H_2O$ (4:1, 5 mL total). 1-Hexyne (49 mg, $6.0 \times 10^{-4}$ mol), Cu(II)$SO_4 \cdot 5H_2O$ (63 mg, $2.5 \times 10^{-4}$ mol), and sodium L-ascorbate (96 mg, $4.8 \times 10^{-4}$ mol) were added sequentially, and the resulting mixture was stirred at room temperature for 24 h. Particles were purified according to reported wash sequence A and dried in vacuo at 75 °C to yield ND-**5b** as a gray powder (24 mg). FT-IR (KBr) $\nu$ ($cm^{-1}$): 3432 (s), 2960 (w, C−H), 2921 (w), 2852 (w), 1735 (w, C═O), 1630 (m, O−H bend; $H_2O$), 1401 (w), 1130 (w), 1022 (w), 954 (w). TGA ($\Delta m$) (150−470 °C): 6.4%. C, 77.81%; H, 1.31%; N, 2.02%.

*4-(4-(Trifluoromethyl)phenyl)-1H-1,2,3-triazole-Terminated Nanodiamond (**6b**).* Following the general procedure, ND-**2b** (31 mg) was suspended in DMF/$H_2O$ (4:1, 5 mL total). 1-Ethynyl-(4-trifluoromethyl)benzene (102 mg, $6 \times 10^{-4}$ mol), Cu(II)$SO_4 \cdot 5H_2O$ (59 mg, $2.4 \times 10^{-4}$ mol), and sodium L-ascorbate (96 mg, $4.8 \times 10^{-4}$ mol) were added sequentially, and the resulting mixture was stirred at room temperature for 22 h. Particles were purified according to reported wash sequence A and dried in vacuo at 75 °C to yield ND-**6b** as a pale yellowish-gray powder (28 mg). FT-IR (KBr) $\nu$ ($cm^{-1}$): 3432 (s), 2921 (w), 2851 (w), 1926 (w), 1752 (w, C═O), 1611 (m, C═C; aryl and O−H bend; $H_2O$), 1403 (w), 1321 (s, C−F; $CF_3$), 1205 (w), 1175 (w), 1107 (m), 1067 (m), 1017 (w), 952 (w), 836 (m, C−H; *p*-disubst benzene), 732 (w), 594 (w), 519 (w). TGA ($\Delta m$) (150−470 °C): 11.8%. C, 73.41%; H, 1.05%; N, 1.73%; F, 4.39%.

*4-Hexadecyl-1H-1,2,3-triazole-Terminated Nanodiamond (**7b**).* Following the general procedure, ND-**2b** (32 mg) was suspended in DMF/$H_2O$ (4:1, 5 mL total). 1-Octadecyne (150 mg, $6.0 \times 10^{-4}$ mol), Cu(II)$SO_4 \cdot 5H_2O$ (65 mg, $2.6 \times 10^{-4}$ mol), and sodium L-ascorbate (94 mg, $4.8 \times 10^{-4}$ mol) were added sequentially, and the resulting mixture was stirred at room temperature for 24 h. Particles were purified according to reported wash sequence A and dried in vacuo at 75 °C to yield **7b** as a brown powder (32 mg). FT-IR (KBr) $\nu$ ($cm^{-1}$): 3439 (m), 2917 and 2850 (C−H), 1752 (w, C═O), 1630 (w, O−H bend; $H_2O$), 1470 (w, C−H; bend), 1401 (w), 718 (w). TGA ($\Delta m$) (150−470 °C): 24.9%. C, 76.25%; H, 4.55%; N, 1.23%.

*4-(Phenanthren-9-yl)-1H-1,2,3-triazole-Terminated Nanodiamond (**8b**).* Following the general procedure, ND-**2b** (28 mg) was suspended in DMF/$H_2O$ (4:1, 5 mL total). 9-Ethynylphenanthrene (119 mg, $5.9 \times 10^{-4}$ mol), Cu(II)$SO_4 \cdot 5H_2O$ (58 mg, $2.3 \times 10^{-4}$ mol), and sodium L-ascorbate (93 mg, $4.7 \times 10^{-4}$ mol) were added sequentially, and the resulting mixture was stirred at room temperature for 21 h. Particles were purified according to reported wash sequence B and dried in vacuo at 75 °C to yield **7b** as a golden-brown powder (18 mg). FT-IR (KBr) $\nu$ ($cm^{-1}$): 3439 (s), 2923 (w), 2851 (w), 1758 (w, C═O), 1630 (m, O−H bend; $H_2O$), 1401 (w), 1384 (w), 890 (w, C−H; deform.), 740 (w, C−H; deform.), 718 (w). TGA ($\Delta m$) (150−470 °C): 10.7%. C, 82.46%; H, 1.34%; N, 1.98%.

## RESULTS AND DISCUSSION

High-purity (0.6% ash content) carboxylic acid ND (Adámas Nanotechnologies) (ND-**1**) synthesized by detonation was used to establish the conditions for decarboxylative azidation. The primary particle size from the supplier was reported to be 4−5 nm with an average aggregate size of ∼130 nm. We substantiated the particle size, diamond structure, and surface area of the starting material by transmission electron microscopy (TEM), selected-area electron diffraction (SAED), and gas adsorption experiments. TEM images of


DOI: 10.1021/acs.langmuir.6b04477
Langmuir XXXX, XXX, XXX−XXX

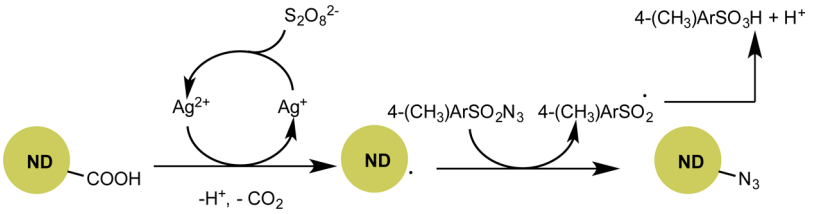


**Figure 1.** Postulated mechanism for the azidation of *carboxylated-ND via decarboxylation and a free radical pathway. (Note that the simplified ND surface structure depicted has additional noncarboxylic acid groups that have been omitted for clarity.) The mechanism is supported by experimental results on small-molecule substrates reported in ref 22.

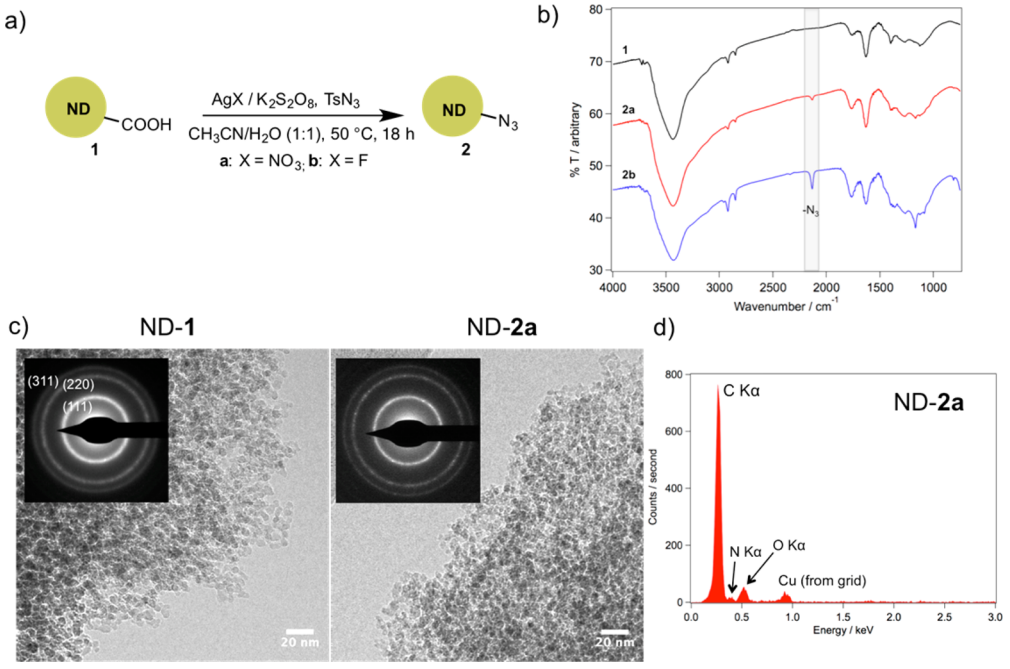


**Figure 2.** (a) Silver-mediated decarboxylation of commercially available detonation powder **1** and conversion to azide-functionalized powders **2a** (with $AgNO_3$) and **2b** (with AgF). (b) FT-IR spectra indicate the presence of $N_3$ groups in **2a** and to a larger extent in **2b**. (c) TEM images of COOH-ND starting material (**1**, left) and $N_3$-terminated-ND (**2a**, right) with SAED patterns (inset), confirming a pure diamond phase. (d) EDS spectrum of ND-**2a** indicating X-ray lines for C, N, and O only, with peaks from Ag and S absent.

ND-**1** confirmed the presence of primary particles in the range of ~4−5 nm (Figure 2C). Large aggregation, as is typical during the drying of detonation nanodiamond, was also observed.[31] SAED of this aggregate was used to confirm the diamond phase as demonstrated by the strong diffraction of (111), (220), and (311) planes (Figure 2C, inset).[32] The specific surface area of the ND-**1** starting material determined from the Langmuir isotherm using the BET method was 296 $m^2\ g^{-1}$ (Figure S1). Because the powder retained a high surface area, further deaggregation beyond sonication was not performed prior to subsequent surface modification experiments.

Direct conversion of carboxylated-ND to azide-ND was initiated by Ag(I)-mediated decarboxylation. The mechanism of decarboxylative azidation is proposed to occur by persulfate-facilitated oxidation of Ag(I) to an active Ag(II) intermediate where radical-based decarboxylation occurs. The remaining alkyl radical then attacks a sulfonyl azide to produce the desired alkyl azide[22] (Figure 1). Our initial attempts toward the decarboxylation of ND-**1** first employed $AgNO_3$ as the Ag(I) source. Briefly, ND-**1** was dispersed in $CH_3CN/H_2O$ (1:1) by bath sonication, and then $AgNO_3$, $K_2S_2O_8$, and tosyl azide were added. The mixture was gently heated (to 50 °C) and stirred for 18 h (Figure 2a). After separating the ND by centrifugation, repeated washing, and subsequent drying, azide-functionalized ND-**2a** was obtained. The azidation reaction to form ND-**2a** was first analyzed by FT-IR (Figure 2b, red trace). A new absorption typical of terminal azide was observed at 2134 $cm^{-1}$. The structural integrity of the diamond core was not compromised during the conversion from carboxylic acid to azide. TEM imaging of ND-**2a** (Figure 2c, right) revealed similar particle sizes and morphology as observed in the starting carboxylated material, and the SAED pattern indicated a pure diamond phase. The energy-dispersive X-ray (EDS) spectrum recorded on a large agglomerate of ND-**2a** (Figure 2d) found only K-edge lines for C, N, and O whereas the Ag L$\alpha$ X-ray line at 2.98 keV and the S K$\alpha$ X-ray line at 2.31 keV were absent. The EDS spectrum therefore indicated that the washing protocol successfully removed the Ag reaction mediator and unreacted or free tosyl azide source and oxidant (both containing sulfur).

Combustion analysis of ND-**2a** indicated a decrease in both carbon and hydrogen contents, suggesting decarboxylation, and a small increase (from 2.26 to 2.32%) in N content, suggesting azidation. This lower-than-anticipated increase in N content despite the formation of azide may result from the simultaneous


DOI: 10.1021/acs.langmuir.6b04477
Langmuir XXXX, XXX, XXX−XXX

Table 1. Elemental Analysis Results and TGA Mass Losses for Detonation Nanodiamond Starting Material (1) and Azide-Functionalized (2a, 2b) Materials

| detonation nanodiamond | % C | % H | % N | TGA mass loss (%) (150−470 °C) |
|---|---|---|---|---|
| ND-**1** (COOH) | 88.49 | 0.86 | 2.26 | 0.5 |
| ND-**2a** ($N_3$, from $AgNO_3$) | 87.23 | 0.76 | 2.32 | 1.4 |
| ND-**2b** ($N_3$, from AgF)[a] | 86.30 | 0.94 | 2.55 | 1.9 |

[a]Average of two experiments where % C = 86.21, 86.39; % H = 0.91, 0.97, and % N = 2.49, 2.61, respectively.

increase in O content in the sample due to the oxidation (from persulfate) of other non-carboxylic acid-containing surface groups. Although $N_3$ groups were observed in **2a**, significant carbonyl groups (C═O, centered at 1763 $cm^{-1}$) relative to azide remained on the surface, as indicated by FT-IR. Note that the second large band at 1630 $cm^{-1}$ is attributed to the O−H bending mode of adsorbed water molecules, commonly found on ND samples even with extensive drying.[33] The use of an alternative azide source (benzenesulfonyl azide) or an increase in reaction time (up to 2 days) failed to improve the loading of azide on the surface relative to the conditions used to generate **2a** (as inferred from FT-IR spectra, not shown).

However, during our screening experiments it was found that AgF (as the Ag(I) source) led to an increase in the number of azide groups on the ND surface. The substitution of $AgNO_3$ for AgF (using conditions that led to **2a**) produced ND-**2b**. The azide IR absorption increased significantly relative to the C═O region (Figure 2b, blue trace). Combustion analysis of ND-**2b** also found an increase in N content to 2.55% (relative to 2.32% for **2a** and 2.26% for **1**). In the case of ND-**2b**, a slight increase in H content and a relatively modest increase in N content over starting ND-**1** is thought to result from concurrent surface group oxidation processes as noted above in ND-**2a** and also from adsorbed tosylic acid generated in the reaction (S═O; $SO_2$ antisym. stretch at 1169 $cm^{-1}$ observed by IR). The mixed surface structure of predominantly azide and oxidized groups currently precludes a calculation of the number of azide groups grafted to the ND surface. Nonetheless, the elemental analysis supports the grafting of azide groups observed by IR. From small-molecule studies previously on 1-adamantanecarboxylic acid, AgF had reactivity similar to that of $AgNO_3$, although it was noted that AgF is more stable than $AgNO_3$ under light.[23] Although light exposure was minimized during azidation in this work, rigorous exclusion was not attempted, which may have contributed to a difference in reactivity with $AgNO_3$. A full exploration of the role of the Ag(I) source in reactivity toward carboxylated nanodiamond is still under investigation.

After successfully establishing Ag-mediated decarboxylation as a route to yield linker-free $N_3$-functionalized ND, our attention next focused on the use of these particles as a general starting material for further surface modification. The ability of azide-functionalized ND-**2b** (containing the largest number of surface $N_3$ groups) to facilitate easy access to more complex materials was demonstrated by treatment with alkynes under standard Cu-catalyzed azide−alkyne cycloaddition (CuAAC) click chemistry conditions (Scheme 2). Azide-ND was suspended in a mixture of DMF/$H_2O$ (4:1) and treated with alkynes with varying side chains, copper(II) sulfate, and sodium L-ascorbate (for the in situ reduction of Cu(II) to active Cu(I)). After 18−24 h of stirring at room temperature and an exhaustive washing purification protocol to remove unbound material, 1-(ND)-1,2,3-triazole adducts **3b**−**8b** were isolated and characterized below as follows. ND surface modification as a result of CuAAC reactivity was verified by FT-IR and

Scheme 2. CuAAC Reactions Used to Generate ND 3b−8b

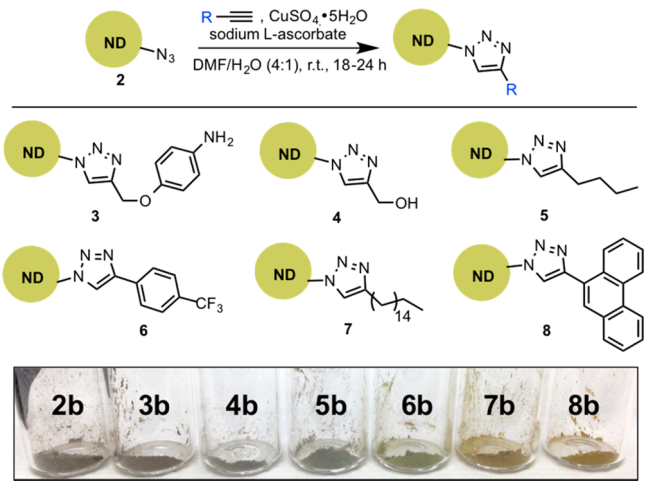


elemental analysis. Surface loadings were estimated from TGA measurements of the mass loss of organic material from the particle surface. Further examination of triazole materials was aided by UV−vis and fluorescence (**8b**) measurements. To our knowledge, NDs **3b**−**8b** are the first examples of dND materials with triazole surface groups directly bound to the carbon core without a spacer group.

In all cases, the FT-IR azide absorption was absent after the reaction, and no remaining absorption from terminal alkyne (C≡C at ca. 2100 $cm^{-1}$ or C−H at ca. 3300 $cm^{-1}$) was found (Figure 3a,b). The 1-(ND)-1,2,3-triazole products in this study varied in structure at the 4 position of the ring, and the side chains ranged from aliphatic (**4b**, **5b**, and **7b**) to aromatic (**3b**, **6b**) and polyaromatic (**8b**). Not surprisingly, alcohol-terminated ND-**4b** has a rather featureless IR spectrum (Figure 3a, gray trace) yet does feature an increased C−O (1020 $cm^{-1}$) stretch. The C−O stretch is likely from a combination of triazole with OH termination and also from remaining surface hydroxyls or ether groups (unaffected by decarboxylative azidation) known to be present on oxidized ND.[21] A small increase in the C $sp^3$−H character of the ND was found for butyl-terminated ND-**5b** (2921 and 2960 $cm^{-1}$, Figure 3a red trace). However, in the case of hexadecyl-terminated ND-**7b**, the C $sp^3$−H signal became much more significant in the IR spectrum (Figure 3a, brown trace), consistent with the formation of a long alkyl group substitution. 4-Methoxyaniline-terminated ND-**3b** produced an FT-IR absorption characteristic of $-NH_3^+$ (from an acidic workup, 1504 $cm^{-1}$) (Figure 3b, blue trace). 4-(Trifluoromethyl)-phenyl terminated ND-**6b** exhibited a strong $-CF_3$ characteristic absorption (1321 $cm^{-1}$). Phenanthrene-terminated ND-**8b** exhibited characteristic C−H absorptions (at 740 and 890 $cm^{-1}$) correlating to the region for the strongest IR absorptions from phenanthrene.[34]

Elemental analyses of materials **3b**−**8b** were performed in order to further support the formation of 1,2,3-triazole linkages



DOI: 10.1021/acs.langmuir.6b04477
Langmuir XXXX, XXX, XXX−XXX

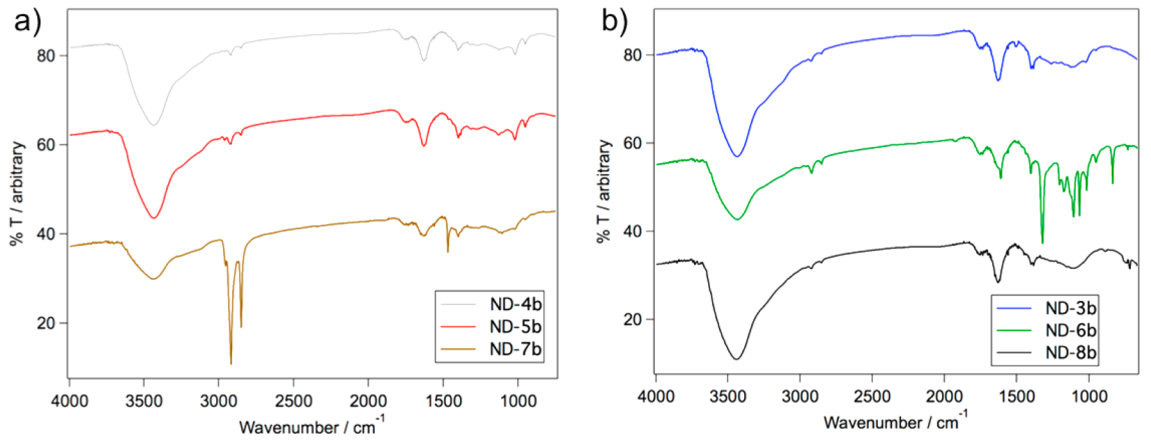


**Figure 3.** (a) Characterization of 4-(aliphatic)-1,2,3-triazole-functionalized ND (**4b**, **5b**, and **7b**) and (b) 4-(aromatic)-1,2,3-triazole-functionalized ND (**3b**, **6b**, and **8b**) by FT-IR.

**Table 2. TGA Mass Losses Due to Organic Groups and Calculated Surface Loadings for 1,2,3-Triazole ND Materials 3b−8b**

| detonation nanodiamond (ND) | % C | % H | % N | % F | TGA mass loss (150−470 °C)/est. surface loading (mmol $g^{-1}$)[a] |
|---|---|---|---|---|---|
| **3b** ((4-$OCH_2$)-aniline) | 80.19 | 1.13 | 2.63 | | 4.3%/0.19 |
| **4b** ($CH_2OH$) | 80.32 | 1.09 | 2.10 | | 4.8%/0.49 |
| **5b**(($CH_2$)$_3CH_3$) | 77.81 | 1.31 | 2.02 | | 6.4%/0.52 |
| **6b** ((4-$CF_3$)-phenyl) | 73.41 | 1.05 | 1.73 | 4.39 | 11.8%/0.56 |
| **7b** (($CH_2$)$_{15}CH_3$) | 76.25 | 4.55 | 1.23 | | 24.9%/0.85 |
| **8b** (phenanthrene) | 82.46 | 1.34 | 1.98 | | 10.7%/0.44 |

[a]Calculated from the molecular weight of 4-(*R*)-1*H*-1,2,3-triazole if fully detached from the surface.

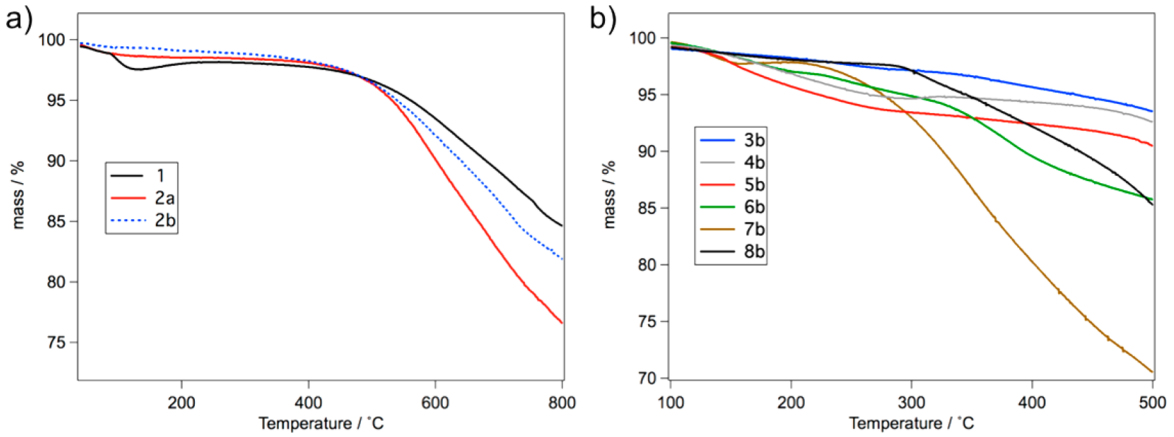


**Figure 4.** (a) TGA data for ND **1** (−COOH, black trace), **2a** (−$N_3$ from $AgNO_3$, red trace), and **2b** (−$N_3$ from AgF, dashed blue trace) collected in an inert atmosphere (He, 10 K $min^{-1}$). (b) TGA data of 1,2,3-triazole-functionalized NDs **3b−8b** collected in an inert atmosphere (He, 10 K $min^{-1}$), showing mass loss due to the presence of surface modification.

obtained by treatment with alkynes under click conditions. Combustion analysis of **3b** found an increase in N content (2.63%) from starting material **2b** (2.55%) due to the presence of an additional amine group. Elemental analysis on ND-**6b** performed by the ion-selective electrode technique determined a F content of 4.39%. Full elemental analysis data for NDs **3b−8b** is given in Table 2.

To obtain more quantitative insight into the extent of surface functionalization of materials **3b−8b** obtained from CuAAC reactions with azide-ND-**2b**, TGA was employed. Because negligible mass loss (0.5%) below 470 °C was observed for starting COOH-ND-**1**, residual unreacted carboxyl, hydroxyl, or other surface groups do not interfere with calculations used to determine estimated surface group loadings of triazole-bound groups. Surface loadings estimated from the mass loss in the region from 150 to 470 °C, where organic surface functional groups typically are removed, ranged from 0.19 to 0.85 mmol $g^{-1}$ (Table 2). Surface loadings for ND containing alkyl side chains in NDs **5b** and **7b** (0.52 and 0.85 mmol $g^{-1}$) were similar to or in some cases exceeded the surface loadings that were previously obtained through borane-treated NDs converted to alkyl ester groups (0.3−0.4 mmol $g^{-1}$)[35] and Fenton-treated ND converted to alkyl ester groups (0.78−2.0 mmol $g^{-1}$).[36] Surface loadings of aryl groups in NDs **3b**, **6b**, and **8b** ranged from 0.19 to 0.56 mmol $g^{-1}$, similar to loadings previously reported with thermally annealed, diazonium treated, CuAAC-modified materials (0.17−0.34 mmol $g^{-1}$)[28] and loadings obtained via amide bond formation and CuAAC-


DOI: 10.1021/acs.langmuir.6b04477
*Langmuir* XXXX, XXX, XXX−XXX

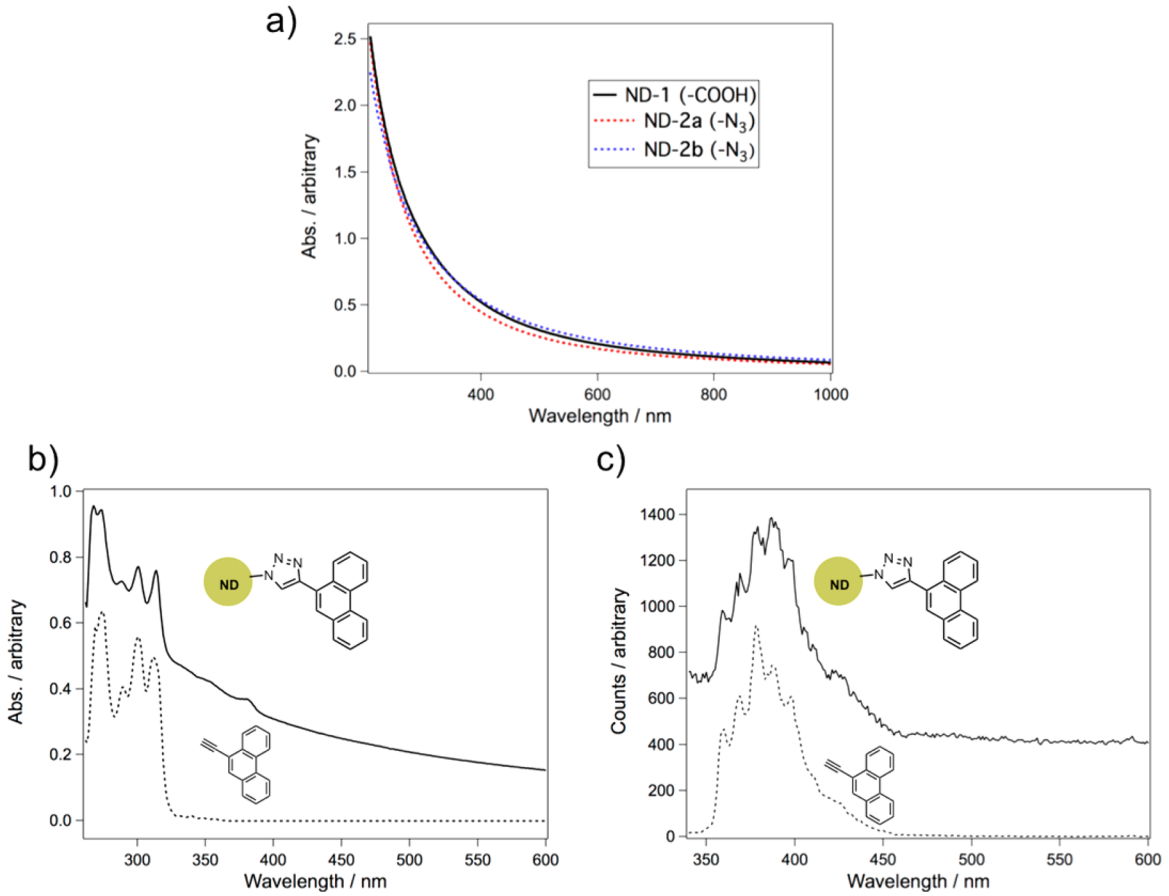


**Figure 5.** (a) UV−vis spectra of ND-**1**, ND-**2a**, and ND-**2b** in $H_2O$. (b) UV−vis spectra of ND-**8b** (top, solid trace) in DMF and free 9-ethynylphenanthrene (bottom, dashed trace). (c) Fluorescence emission spectra of ND-**6b** in DMF (top, solid trace) and free alkyne (bottom, dashed trace) with excitation at 295 nm.

modification (0.54 mmol $g^{-1}$).[27] It should be noted that the region for mass loss of the bound organic surface moieties is not unambiguous because early sublimation of carbon-containing ND core material may occur at ∼450 °C and overlap with the removal of persistent strongly bound surface groups.[37] Furthermore, the presence of nongrafted or adsorbed alkyne moieties cannot be completely ruled out, although no infrared absorptions from free alkynes have been observed on any of the purified triazole-functionalized NDs.

The optical properties of the azide-NDs and 1,2,3-triazole-NDs were also investigated. The absorption spectrum of azide-NDs (**2a** and **2b**) in $H_2O$ was nearly identical to that of starting carboxylated ND **1** (Figure 5a), with scattering from the dispersed ND but with no other specific absorption. However, after CuAAC treatment with polyaromatic 9-ethynylphenanthrene, triazole product ND-**8b** (dispersed in DMF) displayed prominent UV absorption for attached phenanthrene groups (Figure 5b). The attachment of phenanthrene groups to the 4 position of the 1,2,3-triazole ring in ND-**8b** also translated to a measurable fluorescence emission with an excitation wavelength of 295 nm (Figure 5c). It should also be noted that the gray color of ND-**2b** was altered after CuAAC modification to 1,2,3-triazole ND materials **3b**−**8b** depending on the structure of the incoming ligand (Scheme 2). Although the change in color correlates with the attachment of new surface moieties, the precise origin of these color changes has yet to be fully explored.

The straightforward azidation procedure is expected to be valuable for the attachment of a variety of chemically and biologically active groups. Because the surface carboxyl groups represent only a portion of the ND surface, residual alcohol or other hydrophilic surface groups are expected to remain on the surface after decarboxylation, substitution for azide, and postclick treatment, as has been discussed during the decarboxylative fluorination of ND.[21] Therefore, this method results in a multifunctional ND surface where the residual surface groups may promote stability in aqueous and biological environments and the active surface groups installed by click chemistry may be used to tune the reactivity with the particle's external environment.

## CONCLUSIONS

A synthesis method was developed to transform carboxylic acids on ND surfaces directly to azide groups by Ag(I)-mediated decarboxylation. The reported procedure is scalable, occurs in a single step in solution, and yields azide particles of high general utility for subsequent access to more complex surface chemistries via cycloaddition reactions. Specifically, the azide-ND may be treated with a variety of structurally diverse alkynes to yield linker-free, functional 1,2,3-triazole groups on the surface using standard Cu-catalyzed click chemistry conditions. Given that decarboxylation does not affect some of the surface moieties simultaneously present on purified carboxylic acid ND (i.e., alcohols), the resulting surface after click modification is multifunctional. We envision that the


DOI: 10.1021/acs.langmuir.6b04477
Langmuir XXXX, XXX, XXX−XXX

exploitation of these multifunctional characteristics will be particularly advantageous for biological applications where hydrophobic functional species may be appended via a click reaction and the residual remaining surface groups will promote stability under aqueous or buffer conditions. Furthermore, Ag-mediated decarboxylation is a promising approach to pursue for the substitution of other groups such as alkynes directly onto the surface of ND.

## ■ ASSOCIATED CONTENT

### Supporting Information

The Supporting Information is available free of charge on the ACS Publications website at DOI: 10.1021/acs.langmuir.6b04477.

Gas adsorption data for ND-**1** (PDF)

## ■ AUTHOR INFORMATION


### Corresponding Author

*E-mail: marvin.warner@pnnl.gov.

### ORCID

Marvin G. Warner: 0000-0001-9767-5511


### Notes

The authors declare no competing financial interest.

## ■ ACKNOWLEDGMENTS

This work was supported by a laboratory-directed research and development program at Pacific Northwest National Laboratory (PNNL), a laboratory operated by Battelle for the U.S. Department of Energy (DOE) under contract DE-AC06-76RLO 1830.

## ■ REFERENCES


(1) Neitzel, I.; Mochalin, V.; Knoke, I.; Palmese, G. R.; Gogotsi, Y. Mechanical properties of epoxy composites with high contents of nanodiamond. *Compos. Sci. Technol.* **2011**, *71*, 710−716.

(2) Mochalin, V. N.; Shenderova, O.; Ho, D.; Gogotsi, Y. The properties and applications of nanodiamonds. *Nat. Nanotechnol.* **2012**, *7*, 11−23.

(3) Gunawan, M. A.; Hierso, J.-C.; Poinsot, D.; Fokin, A. A.; Fokina, N. A.; Tkachenko, B. A.; Schreiner, P. R. Diamondoids: functionalization and subsequent applications of perfectly defined molecular cage hydrocarbons. *New J. Chem.* **2014**, *38*, 28−41.

(4) Krueger, A.; Lang, D. Functionality is Key: Recent Progress in the Surface Modification of Nanodiamond. *Adv. Funct. Mater.* **2012**, *22*, 890−906.

(5) Danilenko, V. V. Nanodiamonds: Problems and prospects. *J. Superhard Mater.* **2010**, *32*, 301−310.

(6) Pichot, V.; Comet, M.; Fousson, E.; Baras, C.; Senger, A.; Le Normand, F.; Spitzer, D. An efficient purification method for detonation nanodiamonds. *Diamond Relat. Mater.* **2008**, *17*, 13−22.

(7) Krueger, A. The structure and reactivity of nanoscale diamond. *J. Mater. Chem.* **2008**, *18*, 1485−1492.

(8) Chung, P. H.; Perevedentseva, E.; Tu, J. S.; Chang, C. C.; Cheng, C. L. Spectroscopic study of bio-functionalized nanodiamonds. *Diamond Relat. Mater.* **2006**, *15*, 622−625.

(9) Huang, L. C. L.; Chang, H.-C. Adsorption and Immobilization of Cytochrome c on Nanodiamonds. *Langmuir* **2004**, *20*, 5879−5884.

(10) Manus, L. M.; Mastarone, D. J.; Waters, E. A.; Zhang, X.-Q.; Schultz-Sikma, E. A.; MacRenaris, K. W.; Ho, D.; Meade, T. J. Gd(III)-Nanodiamond Conjugates for MRI Contrast Enhancement. *Nano Lett.* **2010**, *10*, 484−489.

(11) Gong, J.; Steinsultz, N.; Ouyang, M. Nanodiamond-based nanostructures for coupling nitrogen-vacancy centres to metal nanoparticles and semiconductor quantum dots. *Nat. Commun.* **2016**, *7*, 11820.

(12) Krüger, A.; Liang, Y.; Jarre, G.; Stegk, J. Surface functionalisation of detonation diamond suitable for biological applications. *J. Mater. Chem.* **2006**, *16*, 2322−2328.

(13) Zhang, X.; Fu, C.; Feng, L.; Ji, Y.; Tao, L.; Huang, Q.; Li, S.; Wei, Y. PEGylation and polyPEGylation of nanodiamond. *Polymer* **2012**, *53*, 3178−3184.

(14) Lin, Y.; Su, D. Fabrication of Nitrogen-Modified Annealed Nanodiamond with Improved Catalytic Activity. *ACS Nano* **2014**, *8*, 7823−7833.

(15) Liu, Y.; Gu, Z.; Margrave, J. L.; Khabashesku, V. N. Functionalization of Nanoscale Diamond Powder: Fluoro-, Alkyl-, Amino-, and Amino Acid-Nanodiamond Derivatives. *Chem. Mater.* **2004**, *16*, 3924−3930.

(16) Lisichkin, G. V.; Korol'kov, V. V.; Tarasevich, B. N.; Kulakova, I. I.; Karpukhin, A. V. Photochemical chlorination of nanodiamond and interaction of its modified surface with C-nucleophiles. *Russ. Chem. Bull.* **2006**, *55*, 2212−2219.

(17) Wang, P.-F.; Wang, X.-Q.; Dai, J.-J.; Feng, Y.-S.; Xu, H.-J. Silver-Mediated Decarboxylative C−S Cross-Coupling of Aliphatic Carboxylic Acids under Mild Conditions. *Org. Lett.* **2014**, *16*, 4586−4589.

(18) Liu, X.; Wang, Z.; Cheng, X.; Li, C. Silver-Catalyzed Decarboxylative Alkynylation of Aliphatic Carboxylic Acids in Aqueous Solution. *J. Am. Chem. Soc.* **2012**, *134*, 14330−14333.

(19) Yin, F.; Wang, Z.; Li, Z.; Li, C. Silver-Catalyzed Decarboxylative Fluorination of Aliphatic Carboxylic Acids in Aqueous Solution. *J. Am. Chem. Soc.* **2012**, *134*, 10401−10404.

(20) Cui, L.; Chen, H.; Liu, C.; Li, C. Silver-Catalyzed Decarboxylative Allylation of Aliphatic Carboxylic Acids in Aqueous Solution. *Org. Lett.* **2016**, *18*, 2188−2191.

(21) Havlik, J.; Raabova, H.; Gulka, M.; Petrakova, V.; Krecmarova, M.; Masek, V.; Lousa, P.; Stursa, J.; Boyen, H.-G.; Nesladek, M.; Cigler, P. Benchtop Fluorination of Fluorescent Nanodiamonds on a Preparative Scale: Toward Unusually Hydrophilic Bright Particles. *Adv. Funct. Mater.* **2016**, *26*, 4134−4142.

(22) Liu, C.; Wang, X.; Li, Z.; Cui, L.; Li, C. Silver-Catalyzed Decarboxylative Radical Azidation of Aliphatic Carboxylic Acids in Aqueous Solution. *J. Am. Chem. Soc.* **2015**, *137*, 9820−9823.

(23) Zhu, Y.; Li, X.; Wang, X.; Huang, X.; Shen, T.; Zhang, Y.; Sun, X.; Zou, M.; Song, S.; Jiao, N. Silver-Catalyzed Decarboxylative Azidation of Aliphatic Carboxylic Acids. *Org. Lett.* **2015**, *17*, 4702−4705.

(24) Johnson, R. G.; Ingham, R. K. The Degradation Of Carboxylic Acid Salts By Means Of Halogen - The Hunsdiecker Reaction. *Chem. Rev.* **1956**, *56*, 219−269.

(25) Köhn, M.; Breinbauer, R. The Staudinger Ligation—A Gift to Chemical Biology. *Angew. Chem., Int. Ed.* **2004**, *43*, 3106−3116.

(26) Lutz, J.-F. 1,3-Dipolar Cycloadditions of Azides and Alkynes: A Universal Ligation Tool in Polymer and Materials Science. *Angew. Chem., Int. Ed.* **2007**, *46*, 1018−1025.

(27) Barras, A.; Szunerits, S.; Marcon, L.; Monfilliette-Dupont, N.; Boukherroub, R. Functionalization of Diamond Nanoparticles Using "Click" Chemistry. *Langmuir* **2010**, *26*, 13168−13172.

(28) Meinhardt, T.; Lang, D.; Dill, H.; Krueger, A. Pushing the Functionality of Diamond Nanoparticles to New Horizons: Orthogonally Functionalized Nanodiamond Using Click Chemistry. *Adv. Funct. Mater.* **2011**, *21*, 494−500.

(29) Romanova, E. E.; Akiel, R.; Cho, F. H.; Takahashi, S. Grafting Nitroxide Radicals on Nanodiamond Surface Using Click Chemistry. *J. Phys. Chem. A* **2013**, *117*, 11933−11939.

(30) Waser, J.; Gaspar, B.; Nambu, H.; Carreira, E. M. Hydrazines and Azides via the Metal-Catalyzed Hydrohydrazination and Hydroazidation of Olefins. *J. Am. Chem. Soc.* **2006**, *128*, 11693−11712.

(31) Krüger, A.; Kataoka, F.; Ozawa, M.; Fujino, T.; Suzuki, Y.; Aleksenskii, A. E.; Vul', A. Y.; Ōsawa, E. Unusually tight aggregation in detonation nanodiamond: Identification and disintegration. *Carbon* **2005**, *43*, 1722−1730.




DOI: 10.1021/acs.langmuir.6b04477
*Langmuir* XXXX, XXX, XXX−XXX

(32) Gruen, D. M. Nanocrystalline Diamond Films. *Annu. Rev. Mater. Sci.* **1999**, *29*, 211−259.
(33) Schmidlin, L.; Pichot, V.; Comet, M.; Josset, S.; Rabu, P.; Spitzer, D. Identification, quantification and modification of detonation nanodiamond functional groups. *Diamond Relat. Mater.* **2012**, *22*, 113−117.
(34) Wu, M. L.; Nie, M. Q.; Wang, X. C.; Su, J. M.; Cao, W. Analysis of phenanthrene biodegradation by using FTIR, UV and GC−MS. *Spectrochim. Acta, Part A* **2010**, *75*, 1047−1050.
(35) Krueger, A.; Boedeker, T. Deagglomeration and functionalisation of detonation nanodiamond with long alkyl chains. *Diamond Relat. Mater.* **2008**, *17*, 1367−1370.
(36) Martín, R.; Heydorn, P. C.; Alvaro, M.; Garcia, H. General Strategy for High-Density Covalent Functionalization of Diamond Nanoparticles Using Fenton Chemistry. *Chem. Mater.* **2009**, *21*, 4505−4514.
(37) Jarre, G.; Heyer, S.; Memmel, E.; Meinhardt, T.; Krueger, A. Synthesis of nanodiamond derivatives carrying amino functions and quantification by a modified Kaiser test. *Beilstein J. Org. Chem.* **2014**, *10*, 2729−2737.



DOI: 10.1021/acs.langmuir.6b04477
*Langmuir* XXXX, XXX, XXX−XXX